Catalytic Removal of Volatile Organic Compounds over Porous Catalysts

Xingtian Zhao, Shaohua Xie, Huanggen Yang, Jiguang Deng and Hongxing Dai*

Beijing Key Laboratory for Green Catalysis and Separation, Key Laboratory of Beijing on Regional Air Pollution Control, Key Laboratory of Advanced Functional Materials, Education Ministry of China, Laboratory of Catalysis Chemistry and Nanoscience, Department of Chemistry and Chemical Engineering, College of Environmental and Energy Engineering, Beijing University of Technology, Beijing 100124, China

Abstract: In this review, we summarize the recent research progress on the preparation and catalytic performance of meso- and macroporous metal oxide or mixed metal oxide (including manganese oxides, cobalt oxides, iron oxides, chromium oxides, and perovskite-type oxides) catalysts and their supported transition metal and noble metal catalysts for the oxidative removal of typical volatile organic compounds (VOCs), which were prepared using the hard-templating and polyvinyl alcohol-protected reduction methods, respectively. Most of these porous catalysts performed well for the addressed reactions, which was associated with their surface areas, adsorbed oxygen species concentrations, low-temperature reducibility, interactions between noble metal or metal oxide and support as well as porous structures. In addition, the perspectives for developing high-performance catalytic materials and novel VOCs removal technologies are also proposed.

Keywords: ordered porous material, metal oxide, perovskite-type oxide, supported catalyst, volatile organic compound removal.

1. INTRODUCTION

Most of volatile organic compounds (VOCs, e.g. formaldehyde, benzene, toluene, and xylene) not only cause a harmful effect on human health, but also lead to generation of secondary air pollutants, such as O_3 and particulate matter (PM2.5). Therefore, VOCs are considered as major components of atmospheric environment pollutants. Catalytic oxidation is generally regarded as one of the most effective and economic pathways for the oxidative removal of VOCs, and the key issue of such a technology is the development of high-performance catalysts. Up to now, a lot of efforts have been made by many research groups on the elimination of VOCs. For example, He and co-workers reported that over the Pt/TiO_2 catalyst, HCHO could be completely oxidized into CO_2 and H_2O at room temperature [1–3]. Huang *et al*. [4] and Hu *et al*. [5] found that the manganese oxide-supported atomic silver catalysts exhibited excellent performance for the complete oxidation of HCHO. Generally speaking, there are two kinds of catalysts for the catalytic removal of VOCs: supported noble metals (e.g. Pt, Pd, and Au) and metal oxides or mixed metal oxides (e.g. MnO_x, CrO_x, CoO_x, FeO_x, and perovskite-type oxides). In addition to the above thermal catalysis on VOCs removal, other methods, such as adsorption, photocatalysis, and biodegradation [e.g., 6-14], have also been used to eliminate the VOCs. Compared to the bulk materials, porous ones possess abundant pores and high surface areas, which are beneficial for the diffusion, adsorption, and activation of the reactants. Therefore, porous materials can exhibit higher catalytic performance. In the past decade, our group's research interests have focused on the development of ordered porous catalysts and their applications in the removal of VOCs. In this review, we summarize the research progress on the preparation, characterization, and catalytic performance for VOCs oxidation of ordered porous catalysts, especially the three-dimensionally ordered mesoporous (3DOMeso) and three-dimensionally ordered macroporous (3DOMacro) catalysts.

2. ORDERED MESOPOROUS METAL OXIDE CATALYSTS

Compared to the ordered mesoporous silica, the non-silicon mesoporous materials, especially transition metal oxides, are difficult to synthesize due to their different compositions and variable chemical valence [15]. There are soft and hard template methods for preparation of ordered mesoporous metal oxides. The soft template method involves in not only the self-assembly and cross-linking action of inorganic precursors and organic molecule templates, but also the interaction among the precursors, templates, and solvents. Due to the presence of variable valence metal

*Address correspondence to this author at the Beijing Key Laboratory for Green Catalysis and Separation, Key Laboratory of Beijing on Regional Air Pollution Control, Key Laboratory of Advanced Functional Materials, Education Ministry of China, and Laboratory of Catalysis Chemistry and Nanoscience, Department of Chemistry and Chemical Engineering, College of Environmental and Energy Engineering, Beijing University of Technology, Beijing 100124, China; Tel: 8610 6739 6118; Fax: 8610 6739 1983; E-mail: hxdai@bjut.edu.cn

E-ISSN: 2410-3624/15

ions and different hydrolysis rates, it is difficult to prepare transition metal oxides with ordered mesoporous structures and good crystallinity *via* the soft template route. For example, Sinha *et al*. [16,17] fabricated 3DOMeso CrO_x with tri-block copolymer F127 as soft template after calcination below 300 ^oC. The ordered mesoporous structure, however, could be totally destroyed when the calcination temperature reached above 500 ^oC.

In order to overcome the drawback of the soft template method, Ryoo and co-workers [18] developed a novel strategy, i.e., the hard template method, to generate ordered mesoporous materials using ordered mesoporous silica or carbon as hard template. The typical procedures of the hard template strategy for preparation of ordered mesoporous metal oxides are as follows: (i) the metal precursor is filled into the mesopores of the hard template, (ii) generation of metal oxide crystals *via* a calcination treatment, and (iii) removal of the hard template. The preparation condition and the type of hard template have a great influence on physicochemical property of the mesoporous metal oxide, including dimension and order degree, pore size, and distribution, pore volume, and surface area, which can result in a great difference in catalytic performance of mesoporous metal oxides for VOCs oxidation. Li and co-workers [19] fabricated the two-dimensionally ordered mesoporous (2DOMeso) Co_3O_4 and 3DOMeso Co_3O_4 using the 2DOMeso SBA-15- and 3DOMeso KIT-6-templating methods, respectively. They found that under the reaction conditions of formaldehyde/O_2 molar ratio = 1/500 and space velocity (SV) = 30,000 mL/(g h), 3DOMeso Co_3O_4 exhibited better catalytic activity than 2DOMeso Co_3O_4 for formaldehyde oxidation. Such a good result was believed to be due to the three-dimensional porous channel structure, larger specific surface area, abundant active surface oxygen species and active Co^{3+} species on the exposed (220) face of 3DOMeso Co_3O_4.

It should be pointed that the key issue for preparation of metal oxides with well-ordered mesopores *via* the hard template route is the full filling of mesopores with the metal precursors. In order to achieve this goal, Dai and co-workers [20–24] have made a lot of attempts. Using KIT-6 as hard template and chromium nitrate as chromium source, 3DOMeso CrO_x was fabricated in an autoclave at 130–350 ^oC *via* a novel solvent-free route [20]. Firstly, the well-ground mixture of KIT-6 and chromium nitrate was heated at 80 ^oC for 4 h. Because chromium nitrate melts at about 60 ^oC, the liquid chromium nitrate could migrate into the mesopores of KIT-6. A further increase in temperature (above 125 ^oC) caused the decomposition of chromium nitrate, and then an increase in the inner pressure of the autoclave, which might be beneficial for the complete filling of mesopores of the template. Under the conditions of toluene (or ethyl acetate)/O_2 molar ratio = 1/400 and SV = 20,000 mL/(g h), the 3DOMeso CrO_x sample obtained at 240 ^oC (Figure **1a**) exhibited good catalytic performance for the complete oxidation of toluene or ethyl acetate: the reaction temperature ($T_{90\%}$) required for achieving a 90% conversion of toluene or ethyl acetate was 234 and 190 ^oC, and the apparent activation energy was 79.8 and 51.9 kJ/mol, respectively. Furthermore, this sample was catalytically stable. After 48 h of on-stream reaction, the mesoporous structure of the used 3DOMeso CrO_x (Figure **1b**) was similar to that of the fresh counterpart. Using KIT-6 and SBA-16 as hard template, and metal nitrate-containing ethanol solution as metal source, 3DOMeso Fe_2O_3 and Co_3O_4 (Figure **1c** and **d**) were fabricated *via* the vacuum-aided hard template route [21,22]. Under the assistance of vacuum, the air encapsulated in mesopores of the hard template could be minimized and the metal precursor solution readily infiltrated into the mesopores of the hard template, as a result a maximization in filling of mesopores could be achieved. Over the 3DOMeso Fe_2O_3 catalyst calcined at 400 ^oC under the conditions of acetone (or methanol)/O_2 molar ratio = 1/20 and SV = 20,000 mL/(g h), the $T_{90\%}$ for acetone and methanol oxidation was 208 and 204 ^oC [21], respectively. The 3DOMeso Co_3O_4 catalyst obtained with KIT-6 as template outperformed its counterpart obtained with SBA-16 as template. Over the former sample at toluene (or methanol)/O_2 molar ratio = 1/20 and SV = 20,000 mL/(g h), the $T_{90\%}$ for toluene and methanol oxidation was 190 and 139 ^oC, and the apparent activation energy was 59.9 and 50.1 kJ/mol [22], respectively. Highly ordered mesoporous MnO_2 and Co_3O_4 (Figure **1e** and **f**) with surface areas of up to 266 and 313 m^2/g were prepared by adopting the SBA-16-templating strategy under ultrasonic irradiation, respectively. It might be a result due to the combined actions: (i) ultrasonic irradiation promoted liquid–solid mass transfer and dispersion of the metal precursors within mesopores of the silica template, and (ii) the effective multistep procedure (impregnation → filtration → washing → calcination) minimized the formation of

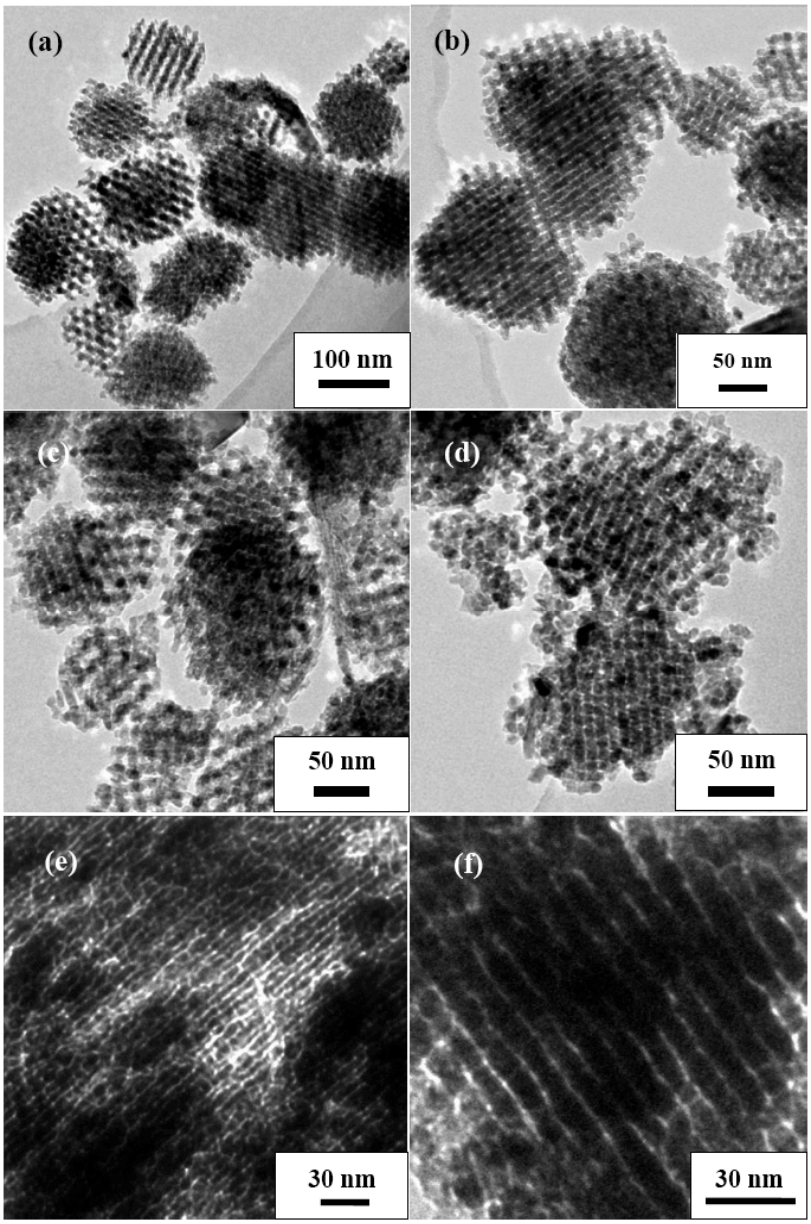

Figure 1: TEM image of (**a**) the fresh ordered mesoporous CrO_x catalyst prepared *via* the solvent free route using KIT-6 as hard template, (**b**) the used ordered mesoporous CrO_x catalyst [20], (**c**) the ordered mesoporous Fe_2O_3 catalyst and (**d**) ordered mesoporous Co_3O_4 catalyst fabricated *via* the vacuum-aided hard template route [21, 22], (**e**) the ordered mesoporous MnO_2 catalyst and (**f**) ordered mesoporous Co_3O_4 catalyst fabricated *via* the SBA-16-templated nanocasting route under ultrasonic irradiation [23].

manganese oxide and cobalt oxide nanoparticles outside the mesopores of the silica template and maximized the filling of the pore channels [23]. Table **1** summarizes the catalytic performance of the porous catalysts for the complete oxidation of typical VOCs. Obviously, compared to the bulk counterpart, the 3DOMeso transition metal oxides showed much better catalytic activities.

Due to the limitation of the hard template method, most of the above mentioned catalysts were single metal oxides with ordered mesopores. In some cases, however, mixed or composite metal oxides might exhibit better performance (including activity, selectivity, stability, and poison tolerance ability), as compared to single metal oxides. Among the mixed metal oxides, perovskite-type oxide (ABO_3) has gained great attention, and been widely used as solid electrolyte, sensor, high-temperature material, solid oxide fuel cell, and catalyst. There are several challenges in the preparation of mesoporous ABO_3 using the hard template method. For example, (i) it is difficult to make the metal precursor migrate into the

Table 1: Catalytic Activities of Ordered Mesoporous and Bulk Metal Oxides for the Oxidation of VOCs

Catalyst	VOC Concentration	VOC/O_2 Molar Ratio	SV (mL/(g h))	Catalytic Activity (^oC)		Ref.
				$T_{50\%}$	$T_{90\%}$	
3DOMeso MnO_2	1000 ppm toluene	1/200	20,000	190	240	[23]
bulk Co_3O_4	1000 ppm toluene	1/20	20,000	200	–	[22]
3DOMeso Co_3O_4	1000 ppm toluene	1/20	20,000	140	180	[22]
bulk Co_3O_4	1000 ppm methanol	1/20	20,000	142	–	[22]
3DOMeso Co_3O_4	1000 ppm methanol	1/20	20,000	105	139	[22]
3DOMeso Co_3O_4	1000 ppm toluene	1/200	20,000	160	200	[23]
bulk Fe_2O_3	1000 ppm acetone	1/20	20,000	235	–	[21]
3DOMeso Fe_2O_3	1000 ppm acetone	1/20	20,000	151	208	[21]
bulk Fe_2O_3	1000 ppm methanol	1/20	20,000	264	–	[21]
3DOMeso Fe_2O_3	1000 ppm methanol	1/20	20,000	170	204	[21]
bulk CrO_x	1000 ppm toluene	1/400	20,000	190	–	[20]
3DOMeso CrO_x	1000 ppm toluene	1/400	20,000	140	234	[20]
bulk CrO_x	1000 ppm ethyl acetate	1/400	20,000	172	–	[20]
3DOMeso CrO_x	1000 ppm ethyl acetate	1/400	20,000	137	190	[20]
3DOMeso CrO_x	500 ppm formaldehyde	1/300	30,000	92	117	[24]
3DOMeso CrO_x	500 ppm acetone	1/300	30,000	75	124	[24]
3DOMeso CrO_x	500 ppm methanol	1/300	30,000	98	130	[24]

mesopores of the hard template, and completely fill the mesopores; (ii) it is hard to control the stoichiometric ratio of *A*- and *B*-site metal ions; and (iii) it is not easy to retain the mesopores during the generation of a perovksite structure because of the requirement of high-temperature (> 600 ^oC) treatment. Due to the advantages in porous structure, surface area, and potential application in catalysis, however, many efforts have been made to fabricate mesoporous ABO_3. With KIT-6 as hard template, Kaliaguine and co-workers [25] prepared mesoporous LaBO_3 (*B* = Mn, Co, Fe) with surface areas of 110−155 m^2/g. Under the conditions of methanol/O_2 = 1/10 and SV = 39,100 h^{-1}, the catalytic activity for methanol oxidation decreased in the order of $LaMnO_3$ > $LaCoO_3$ > $LaFeO_3$. Over the mesoporous $LaMnO_3$ catalyst, the temperature required for complete oxidation of methanol was 150 ^oC, much lower than those (185 ^oC and 220 ^oC) over the bulk $LaMnO_3$ catalysts derived from the reactive grinding and citric acid-complexing methods, respectively. Gao *et al*. [26] fabricated wormhole-like mesoporous $LaFeO_3$ catalyst using SiO_2 nanospheres (ca. 20 nm in size) as template. Under the conditions of toluene/O_2 molar ratio = 1/400 and SV = 20,000 mL/(g h), the mesoporous $LaFeO_3$ catalyst showed a large surface area of 65 m^2/g and good activity with the $T_{50\%}$ and $T_{90\%}$ of 200 and 253 ^oC for toluene oxidation, respectively.

3. ORDERED MESOPOROUS METAL OXIDE SUPPORTED NOBLE METAL NANOCATALYSTS

Loading a proper amount of noble metal or base metal oxide nanoparticles on the surface of disordered or ordered porous metal oxides can improve their catalytic performance. Ying *et al*. [27] found that compared to CeO_2 nanoparticles prepared by the precipitation method, 3DOMeso CeO_2 possessed a smaller particle size, larger surface area, and higher surface oxygen reducible at low temperatures. The 1.7 wt% Au/3DOMeso CeO_2 catalyst exhibited high activity and stability for the complete oxidation of benzene. Under the conditions of benzene/O_2 molar ratio = 1/42 and SV = 15,000 mL/(g h), benzene could be completely oxidized into CO_2 and H_2O at 200 ^oC over 1.7 wt% Au/3DOMeso CeO_2, and a high benzene conversion was maintained at 220 ^oC during 50 h of on-stream reaction, whereas the CeO_2-supported 1.1 wt% Au nanocatalyst suffered severe deactivation due to sintering of the gold nanoparticles. Wang *et al*. [28] pointed out that the preparation method had an influence on pore structure of the support and distribution of active components. The Pd/3DOMeso Co_3O_4 catalyst derived from an *in situ* nanocasting route possessed a more ordered mesostructure and well-dispersed PdO species than its counterpart derived from a post-impregnation route. Under the conditions of *o*-xylene/O_2 = 1/400 and SV = 60,000

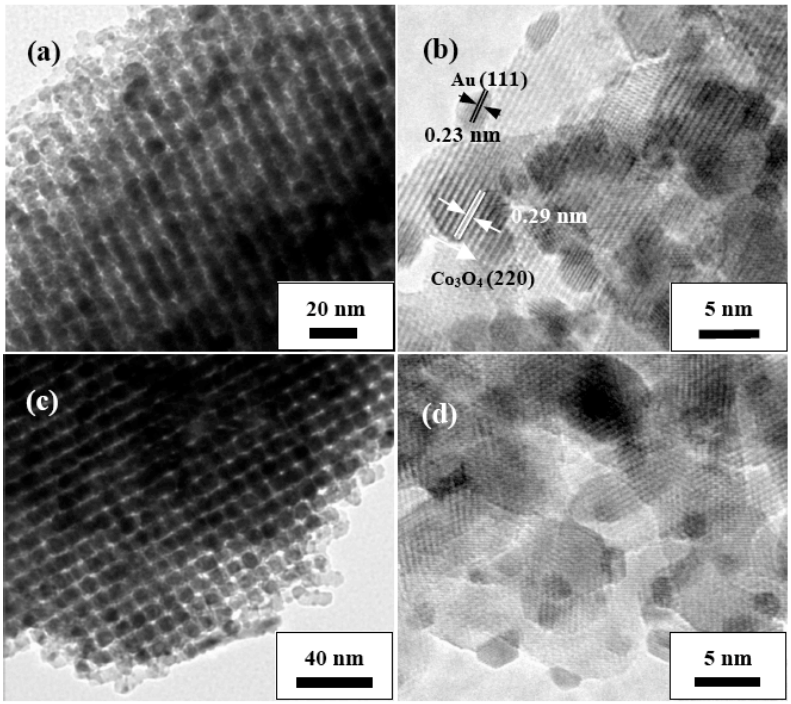

Figure 2: TEM images of (a, b) 3.7 wt% Au/3DOMeso Co_3O_4 and (c, d) 6.5 wt% Au/3DOMeso Co_3O_4 [29].

mL/(g h), the Pd/3DOMeso Co_3O_4 catalyst obtained by the *in situ* nanocasting method exhibited better activity for *o*-xylene oxidation, with the $T_{50\%}$ and $T_{90\%}$ of 193 and 204 °C, respectively. The addition of 1 vol% H_2O and 1000 ppm CO_2 to the feedstock exerted no obvious effects on *o*-xylene conversion, indicating that the Pd/3DOMeso Co_3O_4 catalyst obtained by the *in situ* nanocasting method was highly stable and resistant to H_2O and CO_2. Using the KIT-6-templating and polyvinyl alcohol-protected colloidal deposition methods, Liu *et al*. [29] prepared the *x*Au/3DOMeso Co_3O_4 (*x* = 3.7, 6.5, 9.0 wt%) catalysts (Figure **2**). Under the conditions of CO/O_2 molar ratio = 1/20 and SV = 60,000 mL/(g h) or VOCs/O_2 molar ratio = 1/400 and SV = 20,000 mL/(g h), the 6.5 wt% Au/3DOMeso Co_3O_4 catalyst showed excellent performance for the oxidation of carbon monoxide, benzene, toluene, and *o*-xylene: the $T_{90\%}$ was −45, 189, 138, and 162 °C, respectively. For toluene oxidation, addition of 3.0 vol% water vapor did not affect the catalytic activity of 6.5 wt% Au/3DOMeso Co_3O_4 at a temperature above 160 °C (Figure **3a**). At a higher temperature, Co_3O_4 with stronger lattice oxygen mobility was more facile in activating oxygen molecules, and the adsorption of oxygen was stronger than that of water. When the temperature was below 140 °C, however, addition of 3.0 vol% water vapor caused a stronger adsorption of water molecules on the metal oxide support than that of oxygen molecules, and then decreased the catalytic activity. Introduction of 10.0 vol% CO_2 to the feedstock led to a decrease (by 30%) in activity of the 6.5 wt% Au/3DOMeso Co_3O_4 catalyst (Figure **3b**). The negative effect of CO_2 addition was due to the fact that the surface active sites on 6.5 wt% Au/3DOMeso Co_3O_4 were gradually covered by the carbonate species accumulated during the reaction, which would undermine the activation adsorption of oxygen and/or toluene. After the used catalyst was treated in O_2 at 300 °C for 1 h, the formed carbonate species decomposed completely, with the surface active sites being recovered. Furthermore, gold nanoparticles were highly dispersed on the mesoporous Co_3O_4 surface, which could effectively suppress the chemisorption of SO_2. Therefore, the 6.5 wt% Au/3DOMeso Co_3O_4 sample possessed a good SO_2 tolerance ability (Figure **3c**). Ma *et al*. [30] fabricated 3DOMeso Co_3O_4 with the major exposed active (110) facets, and found that the 3DOMeso Co_3O_4 catalyst was significantly more active for ethylene oxidation than the Co_3O_4 nanosheets with the most exposed (112) facets prepared by the precipitation method. These authors believed that the (110) crystal facet of Co_3O_4 played an essential role in determining the catalytic performance. Furthermore, the 2.5 wt% Au/3DOMeso Co_3O_4 catalyst possessed stable, highly dispersed, and exposed gold sites, rendering it to show a 76% conversion of ethylene at 0 °C at ethylene/O_2 = 1/4410 and SV = 14,400 mL/(g h).

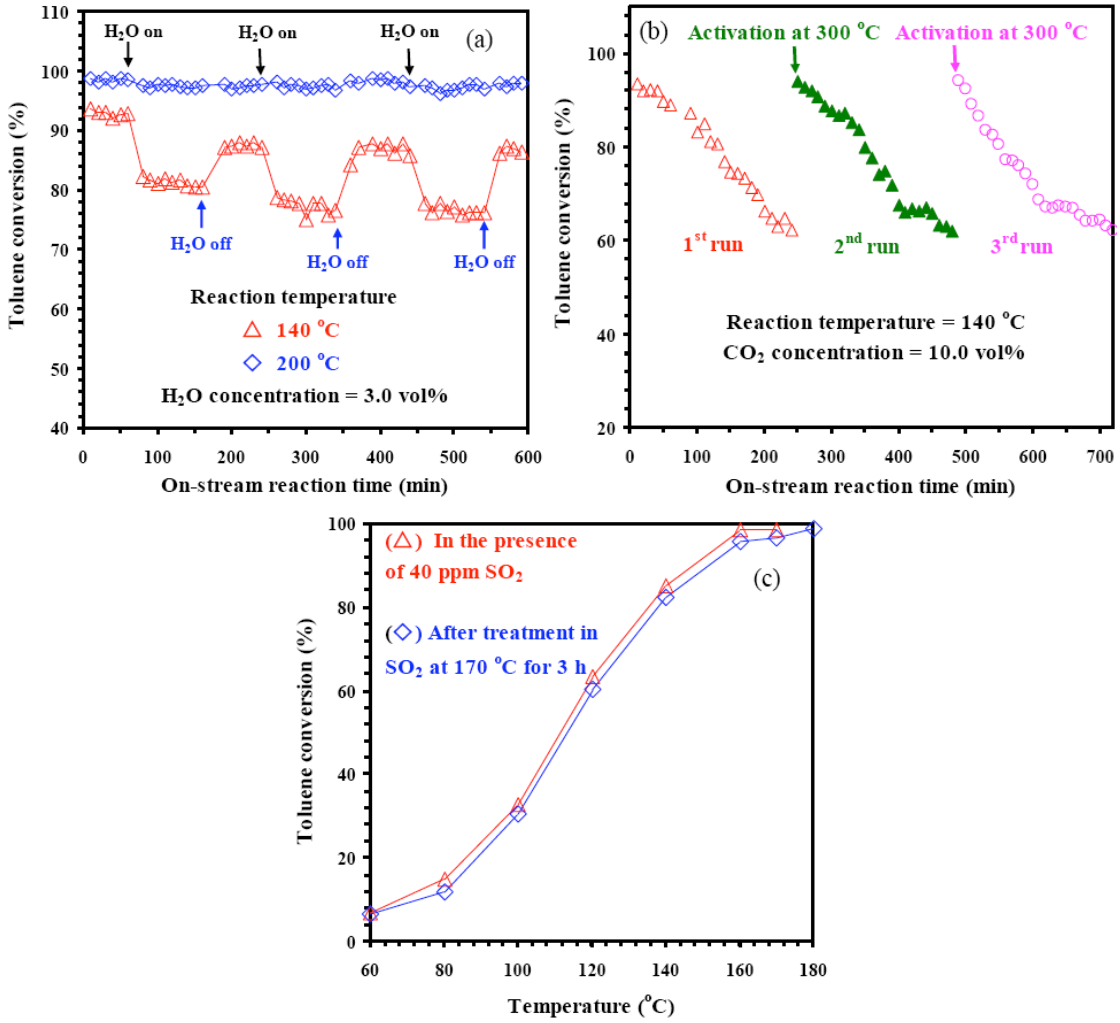

Figure 3: Effect of (a) water vapor, (b) CO_2, and (c) SO_2 on toluene conversion over the 6.5 wt% Au/3DOMeso Co_3O_4 catalyst at toluene/O_2 molar ratio = 1/400 and SV = 20,000 mL/(g h) [29].

4. THREE-DIMENSIONALLY ORDERED MACRO-POROUS METAL OXIDE CATALYSTS

Compared to the ordered mesoporous materials, three-dimensionally ordered macroporous (3DOMacro) materials possess larger pore sizes (> 50 nm), which are beneficial for diffusion of big molecules and can be used as filtration and separation materials, catalyst supports, electrode materials, thermal insulation materials, supports for immobilized cells, etc. Up to now, the colloidal crystal template method is one of the most popular strategies for preparation of 3DOMacro materials. The typical procedures include: (i) synthesizing well-arrayed colloidal crystal microspheres, such as microspheres of polystyrene (PS), polymethyl methacrylate (PMMA), silica, and carbon; (ii) filling the voids of the colloidal crystal template with metal precursors; and (iii) removing the template [31]. Before removal of the template by calcination or extraction, the metal precursors undergo a series of chemical transformations in the voids of the colloidal crystal template. Therefore, the metal precursors and solvent should satisfy the following conditions: (i) in order to keep the well-arrayed structure, the surface of the hard template can be completely wetted by the solvent, whereas the hard template can not be dissolved; (ii) the solubility of the metal precursor in the solvent should be high enough for the purposes of completely filling the voids and then generation of primary 3DOMacro structure with well mechanical strength; and (iii) if the hard template has to be removed *via* calcination, the melt temperature of the metal precursor and the intermediate product derived from the metal precursors should be higher than the glassy temperature of the hard template.

Zhang and co-workers [32−35] fabricated 3DOMacro CeO_2, Au/3DOMacro CeO_2, 3DOMacro CeO_2–Co_3O_4, and Au/3DOMacro CeO_2–Co_3O_4 by the colloidal crystal template method. Due to the shrinkage of the PS microsphere template during the calcination

process, the pore sizes of 3DOMacro CeO_2 prepared with 200, 400, 600, and 800 nm PS microspheres were about 80, 130, 240, and 280 nm, respectively. The Au/3DOMacro CeO_2 catalyst performed better than the Au/bulk CeO_2 catalyst at $HCHO/O_2$ molar ratio = 1/350 and SV = 60,000 mL/(g h), because the 3DOMacro structure with interconnected networks of spherical voids provided benefits of less aggregation and good distribution of Au nanoparticles. The Au/3DOMacro CeO_2 catalyst with a macropore size of 80 nm performed the best, and HCHO could be completely oxidized into CO_2 and H_2O at 75 ^oC [32]. The synergistic effect between CeO_2 and Co_3O_4 accelerated the migration of surface active oxygen species, thus enhancing the catalytic activity of 2.26 wt% Au/3DOMacro CeO_2–Co_3O_4 (CeO_2/Co_3O_4 molar ratio = 2.5:1.0), over which HCHO could be totally oxidized into CO_2 and H_2O at 39 ^oC at $HCHO/O_2$ molar ratio = 1/350 and SV = 15,000 mL/(g h) [35]. Based on the characterization results, these authors concluded that oxidation of HCHO over Au/3DOMacro CeO_2 was mainly catalyzed by the ionic Au^{3+} species. The interaction of Au^0 and CeO_2 generated Au^{3+} and Ce_2O_3. During the adsorption and activation processes of HCHO on the surface of CeO_2, active oxygen might be transferred from Au_2O_3 to HCHO, generating HCOOH and Au^0. Further transfer of active oxygen to HCOOH caused HCOOH to convert into CO_2 and H_2O. Although carbonate and hydrocarbonate species might be formed due to the incomplete oxidation of HCOOH, the generated carbonate and hydrocarbonate species were difficult to block the active sites of Au/3DOMacro CeO_2 with large and open macroporous structures [33]. As we know, Pd alloyed with Au can enhance the catalytic activity. Recently, Xie *et al*. [36] investigated the catalytic performance of *x*AuPd/3DOMacro Co_3O_4 (*x* = 0.50–1.99 wt% and Au/Pd mass ratio = 1:1) for the complete oxidation of toluene, and found that the 3DOMacro Co_3O_4-supported Au–Pd catalysts performed much better than the supported single Au or Pd catalysts, with the 1.99 wt% AuPd/3DOMacro Co_3O_4 catalyst showing the best performance: the $T_{50\%}$ and $T_{90\%}$ were 164 and 168 ^oC at toluene/O_2 molar ratio = 1/400 and SV = 40,000 mL/(g h), respectively. In addition, the 3DOMacro Co_3O_4-supported Au–Pd catalyst also exhibited better catalytic stability and stronger moisture-tolerant ability than the supported Au or Pd catalyst. These authors believed that better oxygen activation ability and stronger noble metal–3DOMacro Co_3O_4 interaction were responsible for the excellent catalytic performance of 1.99 wt% AuPd/3DOMacro Co_3O_4.

Recently, hierarchical porous (e.g. macro-/mesoporous) materials have gained much attention due to their applications in the fields of energy storage and conversion, catalysis, filtration, sensor, and medicines. Using the soft and hard dual template method, Dai and co-workers generated 3DOMacro MgO, 3DOMacro Al_2O_3, 3DOMacro $Ce_{1-x}Zr_xO_2$, 3DOMacro Fe_2O_3, and 3DOMacro Co_3O_4 with mesoporous or nanovoid-like crystalline walls [37–39]. Take the preparation of 3DOMacro Fe_2O_3 with nanovoid-like crystalline walls as an example, surfactant P123 (tri-block copolymers $EO_{20}PO_{70}EO_{20}$) played an important role in generation of nanovoids. With the gradual evaporation of the solvent (ethanol, methanol or ethylene glycol) upon drying, the concentration of P123 rose to a value higher than the critical micelle concentration, and favored the formation of micelles in a disordered array *via* interaction of the Fe precursor with the surfactant, hence resulting in macropore skeletons with nanovoids. Under the conditions of toluene/O_2 molar ratio = 1/400 and SV = 20,000 mL/(g h) for toluene oxidation, the $T_{50\%}$ and $T_{90\%}$ were 240 and 288 ^oC over the 3DOMacro Fe_2O_3 catalyst with nanovoids, whereas 288 and 340 ^oC over the 3DOMacro Fe_2O_3 catalyst without nanovoids, respectively. It is apparent that the presence of a hierarchical porous structure greatly improved the catalytic activity of Fe_2O_3 [38].

As mentioned above, ABO_3 has wide applications in catalysis. In the past ten years, Dai and co-workers have prepared polycrystalline $La_{1-x}Sr_xMO_3$ (*M* = Mn, Co, Fe) nanoparticles [40–42] with high surface areas by coupling the methods of citric acid complexing and hydrothermal synthesis, and single-crystalline $La_{1-x}Sr_xCoO_3$ nanowires/nanorods [43] and $La_{1-x}Sr_xMnO_3$ microcubes [44, 45] *via* the hydrothermal route. The as-obtained poly- or single-crystalline ABO_3 micro- or nanoparticles exhibited good catalytic activities for the oxidation of VOCs. In order to further enhance the performance of ABO_3 for VOCs removal, Dai and co-workers prepared 3DOMacro ABO_3-related catalysts. On the basis of the strategy developed by Ueda and co-workers [46], Dai and co-workers developed a dual (soft and hard) template method for preparation of 3DOMacro ABO_3 with mesopores or nanovoids on the macroprous walls. The typical procedures of the method include: (i) preparation of PMMA microspheres *via* an emulsifier-free emulsion polymerization approach; (ii) generation of ordered arrays of PMMA microspheres (i.e. the PMMA colloidal crystal template) according to the water floating

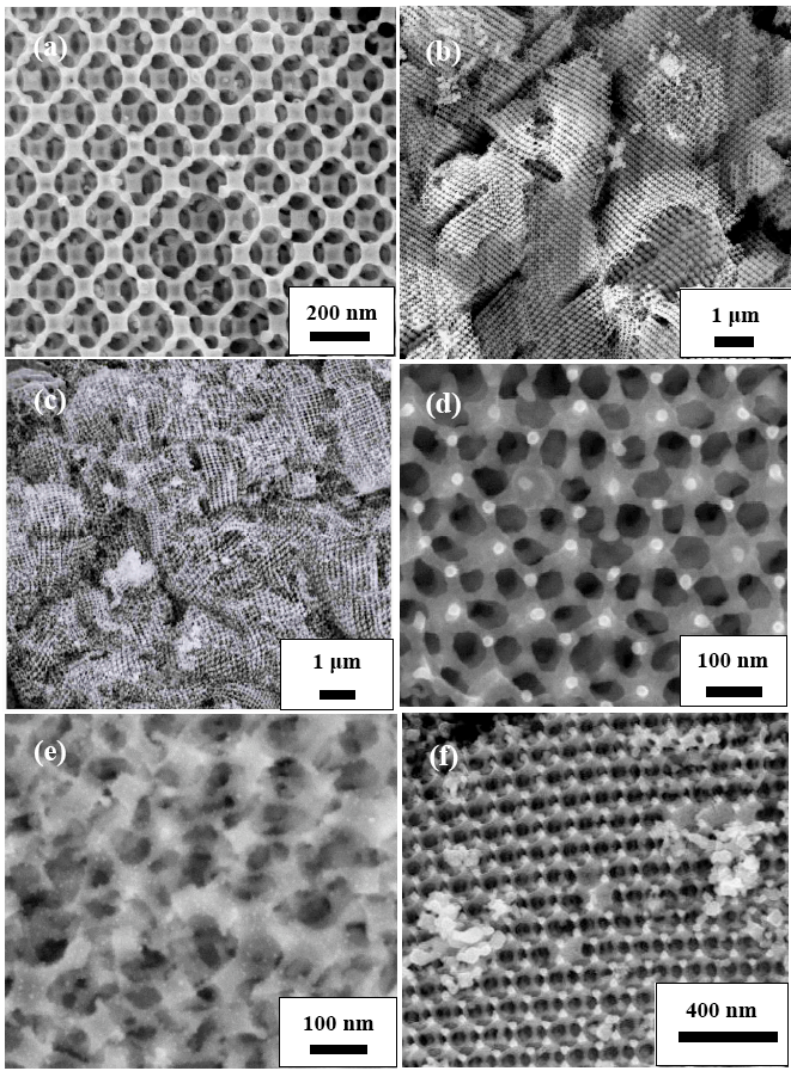

Figure 4: SEM images of (**a**) 3DOMacro $LaMnO_3$ [51], (**b**) 3DOMacro $La_{0.6}Sr_{0.4}MnO_3$ [52], (**c**) 6 wt% CoO_x/3DOMacro $Eu_{0.6}Sr_{0.4}FeO_3$ [53], (**d**) 8 wt% CoO_x/3DOMacro $La_{0.6}Sr_{0.4}CoO_3$ [54], (**e**) 6.4 wt% Au/3DOMacro $La_{0.6}Sr_{0.4}MnO_3$ [52], and (**f**) 5.92 wt% Au/8 wt% MnO_x/3DOMacro $La_{0.6}Sr_{0.4}MnO_3$ [55].

strategy; (iii) preparation of the homogeneous solution consisting of anhydrous methanol, polyethylene glycol (PEG) and water, in which metal precursor, citric acid, and surfactant (e.g., P123, F127, lysine, tryptophan or xylitol) were totally dissolved; (iv) a certain amount of the PMMA colloidal crystal template was soaked in the homogeneous solution, the excess solution was removed from the impregnated PMMA colloidal crystals by vacuum filtration, and the obtained sample was dried in air at room temperature; and (v) calcination treatments were divided into two steps: first in N_2 at a low temperature (300 ^oC) and then in air at a high temperature (750 ^oC) in a tubular furnace. The glassy temperature, decomposition temperature, and oxidation temperature of PMMA in air was about 130, 290, and 370 ^oC, respectively. The PMMA-containing metal precursor was first calcined in N_2 at 300 ^oC, possibly leading to the partial carbonization of PMMA, the as-resulted amorphous carbon could act as a hard template to prevent macro-/mesoporous structure from collapsing before the polymer template was completely oxidized at high temperatures, thus beneficial for the preservation of 3DOMacro-structured ABO_3. Shown in Figures **4** and **5** are the typical SEM and TEM images of the 3DOMacro ABO_3-related catalysts, respectively. It should be pointed out that, in addition to 3DOMacro ABO_3, 3DOMacro $BiVO_4$ [47] and 3DOMacro $InVO_4$ [48] could also be prepared *via* the mentioned dual template route. Interestingly, addition of EG into PEG-containing solution was favorable for generation of hollow spherical $LaMO_3$ and solid spherical MO_x (M = Mn, Co) (Figure **6**) [49]. After precisely adjusting the concentration of metal precursor and PEG, chain-like ordered macroporous $LaMnO_3$ could be obtained (Figure **7**) [50].

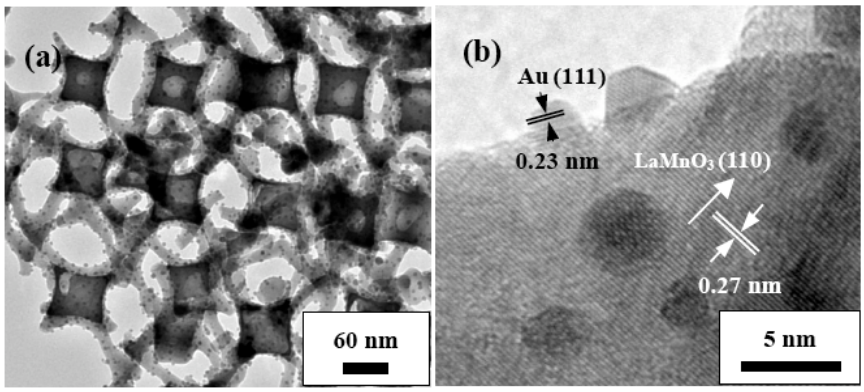

Figure 5: TEM images of 6.4 wt% Au/3DOMacro $La_{0.6}Sr_{0.4}MnO_3$ [52].

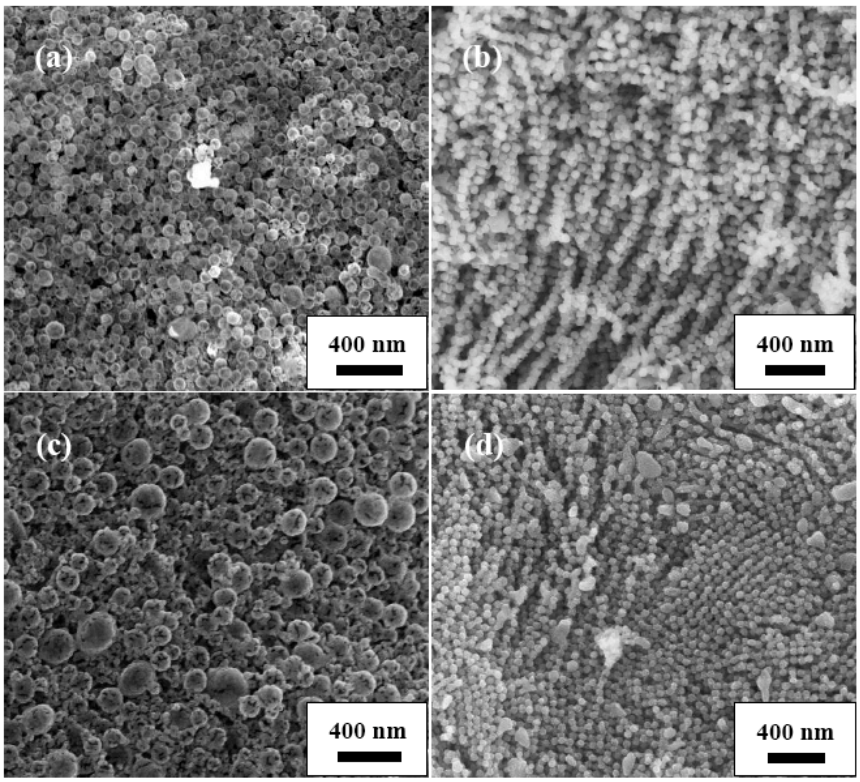

Figure 6: SEM images of (**a**) hollow spherical $LaMnO_3$, (**b**) solid spherical Mn_2O_3, (**c**) hollow spherical $LaCoO_3$, and (**d**) solid spherical Co_3O_4 [49].

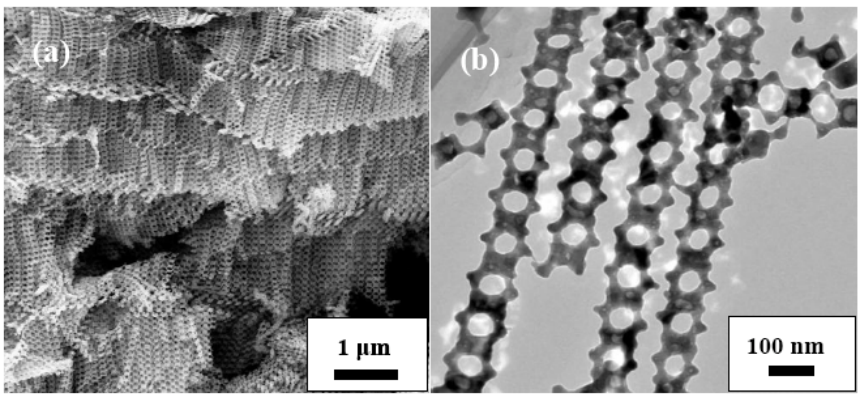

Figure 7: (a) SEM and (b) TEM images of chain-like macroporous $LaMnO_3$ [50].

Compared to the bulk $LaMnO_3$, 3DOMacro $LaMnO_3$ showed a higher catalytic activity for toluene oxidation. Under the conditions of toluene/O_2 molar ratio = 1/400 and SV = 20,000 mL/(g h) (hereinafter referred to the given conditions), $T_{50\%}$ and $T_{90\%}$ over 3DOMacro $LaMnO_3$ were 222 and 243 °C [51,56], respectively. As we know, partial substitution of *A*- and/or *B*-site elements (e.g. $A_{1-x}A'_xBO_3$, $AB_{1-y}B'_yO_3$ and $A_{1-x}A'_xB_{1-y}B'_yO_3$) could enhance the catalytic performance of ABO_3. Under the given conditions, the sequence in catalytic performance for toluene oxidation over 3DOMacro $Eu_{1-x}Sr_xFeO_3$ (x = 0, 0.4, 1) decreased in the order of $Eu_{0.6}Sr_{0.4}FeO_3$ > $SrFeO_3$ > $EuFeO_3$, and the $T_{50\%}$ and $T_{90\%}$ over 3DOMacro $Eu_{0.6}Sr_{0.4}FeO_3$ were 278 and 305 °C [57–59], and over 3DOMacro $La_{0.6}Sr_{0.4}Fe_{0.8}Bi_{0.2}O_3$ were 220 and 242 °C (which were 50 and 70 °C lower than those over 3DOMacro $La_{0.6}Sr_{0.4}FeO_3$ [60,61]), respectively. In order to investigate the synergistic effect between the metal oxide and porous support, Dai and co-workers prepared the MO_y/3DOMacro $A_{1-x}A'_xBO_3$ ($M \neq B$ or M = B) catalysts and evaluated their catalytic performance for VOCs oxidation. Using the incipient wetness impregnation method, the 1–10 wt% CoO_x/3DOMacro $Eu_{0.6}Sr_{0.4}FeO_3$ catalysts were fabricated. Under the given conditions, the $T_{50\%}$ and $T_{90\%}$ over 3 wt% CoO_x/3DOMacro $Eu_{0.6}Sr_{0.4}FeO_3$ were 251 and 270 °C (which were 27 and 35 °C lower than those over 3DOMacro $Eu_{0.6}Sr_{0.4}FeO_3$ [53,62]), respectively. The 2–10 wt% CoO_x/3DOMacro $La_{0.6}Sr_{0.4}CoO_3$ [54] and 5–16 wt% MnO_x/3DOMacro $LaMnO_3$ [63] catalysts were prepared *via* the one-step route (i.e., the *in situ* strategy). Under the given conditions, *in situ* loading a small amount of CoO_x or MnO_x nanoparticles on the 3DOMacro support could effectively improve the catalytic activity for VOCs oxidation, and the 8 wt% CoO_x/3DOMacro $La_{0.6}Sr_{0.4}CoO_3$ and 12 wt% MnO_x/3DOMacro $LaMnO_3$ catalysts exhibited excellent catalytic performance.

As mentioned above, the porous metal oxide-supported noble metal nanocatalysts were highly efficient for the removal of VOCs. Therefore, Dai and co-workers prepared the 1.54–7.63 wt% Au/3DOMacro $LaCoO_3$ [64] and 3.4–7.9 wt% Au/3DOMacro $La_{0.6}Sr_{0.4}MnO_3$ [52] catalysts using the gas bubble-assisted polyvinyl alcohol-protected reduction method. Under the given conditions, the $T_{50\%}$ and $T_{90\%}$ over 6.4 wt% Au/3DOMacro $La_{0.6}Sr_{0.4}MnO_3$ were 150 and 170 °C, respectively. After 100 h of on-stream toluene oxidation reaction at 170 °C, no significant loss in activity was observed over this catalyst. Furthermore, the crystal structure, surface composition, and 3DOMacro structure of the used 6.4 wt% Au/3DOMacro $La_{0.6}Sr_{0.4}MnO_3$ catalyst were rather similar to those of the fresh catalyst. That is to say, the 6.4 wt% Au/3DOMacro $La_{0.6}Sr_{0.4}MnO_3$ catalyst was catalytically durable under the adopted reaction conditions. When the temperature was 170 °C, addition of a small amount (2.5 vol%) of water vapor decreased the activity of 6.4 wt% Au/3DOMacro $La_{0.6}Sr_{0.4}MnO_3$ (toluene conversion dropped from 90 to 80%). Such a negative effect on activity resulted from moisture introduction could be suppressed with a rise in temperature. In addition, the deactivation due to competitive adsorption of H_2O and toluene or O_2 molecules was reversible [52]. Table **2**

Table 2: Catalytic Activities and Activation Energies (E_a) for Toluene Oxidation over the As-Prepared 3DOMacro ABO_3 Catalysts under the Conditions of Toluene Concentration = 1000 ppm, Toluene/O_2 Molar Ratio = 1/400 and SV = 20,000 mL/(g h)

Catalyst	Catalytic Activity (°C)		E_a (kJ/mol)	Ref.
	$T_{50\%}$	$T_{90\%}$		
3DOMacro $LaMnO_3$	222	243	58	[51]
3DOMacro $SrFeO_3$	292	340	–	[57]
3DOMacro $EuFeO_3$	322	353	96.0	[59]
3DOMacro $Eu_{0.6}Sr_{0.4}FeO_3$	278	305	81.1	[59]
3DOMacro $La_{0.6}Sr_{0.4}FeO_3$	271	312	–	[60]
3DOMacro $La_{0.6}Sr_{0.4}Fe_{0.8}Bi_{0.2}O_3$	220	242	45.9	[61]
3 wt% Co_3O_4/3DOMacro $Eu_{0.6}Sr_{0.4}FeO_3$	251	270	72.3	[53]
3DOMacro $La_{0.6}Sr_{0.4}CoO_3$	240	260	57.8	[54]
8 wt% Co_3O_4/3DOMacro $La_{0.6}Sr_{0.4}CoO_3$	210	227	43.3	[54]
12 wt% MnO_x/3DOMacro $LaMnO_3$	193	215	61	[63]
3DOMacro $LaCoO_3$	217	231	38.6	[64]
7.63 wt% Au/3DOMacro $LaCoO_3$	188	202	31.4	[64]
3DOMacro $La_{0.6}Sr_{0.4}MnO_3$	203	219	59	[52]
6.4 wt% Au/3DOMacro $La_{0.6}Sr_{0.4}MnO_3$	150	170	44	[52]

summarizes the catalytic activities for toluene oxidation over the 3DOMacro ABO_3-related catalysts. Based on the characterization results and activity data, it is concluded that the high catalytic performance was associated with the surface area, adsorbed oxygen species concentration, low-temperature reducibility, interaction between noble metal or metal oxide and support as well as the porous structure of the catalyst. It is observed from Table **2** that a catalyst with a better activity showed a lower activation energy.

5. CONCLUSIVE REMARKS AND PERSPECTIVE

In summary, the 3DOMeso- or 3DOMacro-structured manganese oxides, cobalt oxides, iron oxides, chromium oxides, and perovskite-type oxides and preparation and their supported transition metal or noble metal catalysts can be fabricated using the hard-templating and PVA-protected reduction methods. Most of the porous catalytic materials showed high performance for the oxidative removal of typical VOCs, which was associated with their surface areas, adsorbed oxygen species concentrations, low-temperature reducibility, interactions between noble metal or metal oxide and support as well as porous structures.

Although a great progress has been achieved on the preparation and catalytic applications of ordered porous metal oxides for the removal of VOCs, there are still some challenges that should be faced in future work.

(i) In terms of methods for preparation of ordered meso- or macroporous metal oxide catalysts, the hard template method might be an appropriate strategy. However, the drawbacks of this method are obvious. For example, the yield of the target product is very low, the repeatability is poor, and the exposed ratio of active crystal facets is hard to control. Furthermore, it is difficult to amplify in a large scale. Therefore, it is highly desired to develop soft template methods or other novel methods without use of a template for preparation of ordered porous metal oxide catalysts with more active crystal facets being exposed on the surface.

(ii) It is necessary to further elucidate the catalytic mechanisms of ordered porous metal oxide catalysts for the oxidative removal of VOCs. In the presence of single- or multi-component VOCs, clarifying the issues, such as diffusion, adsorption, activation, and reaction, would be of importance in designing and preparing novel and high-efficiency catalytic materials.

(iii) It is highly desirable to develop the coupling technology for effective removal of VOCs with a wide range of VOC concentrations. Different methods, such as adsorption, plasma, heterogeneous catalysis, photocatalysis, and biodegradation, have their unique advantages. Utilization of the coupling technology that combines the advantages of the above methods would guarantee a high efficiency in removing VOCs.

ACKNOWLEDGEMENTS

This work was supported by the Natural Science Foundation of China (21103005 and 21377008), Natural Science Foundation of Beijing Municipality (2132015), and the Doctoral Fund of the Ministry of Education of China (20111103120006).

REFERENCES

[1] Zhang CB, He H and Tanaka K. Perfect catalytic oxidation of formaldehyde over a Pt/TiO_2 catalyst at room temperature. Catal Commun 2005; 6: 211-214. http://dx.doi.org/10.1016/j.catcom.2004.12.012

[2] Zhang CB, He H and Tanaka K. Catalytic performance and mechanism of a Pt/TiO_2 catalyst for the oxidation of formaldehyde at room temperature. Appl Catal B: Environ 2006; 65: 37-43. http://dx.doi.org/10.1016/j.apcatb.2005.12.010

[3] Zhang CB, Liu FD, Zhai YP, Ariga H, Yi Y nad Liu YC, *et al*. Alkali-metal-promoted Pt/TiO_2 opens a more efficient pathway to formaldehyde oxidation at ambient temperatures. Angew Chem Int Ed 2012; 51: 9628-9632. http://dx.doi.org/10.1002/anie.201202034

[4] Huang ZW, Gu X, Cao QQ, Hu PP, Hao JM and Li JH, *et al*. Catalytically active single-atom sites fabricated from silver particles. Angew Chem Int Ed 2012; 51: 4198-4203. http://dx.doi.org/10.1002/anie.201109065

[5] Hu PP, Huang ZW, Amghouz Z, Makkee M, Xu F and Kapteijn F, *et al*. Electronic metal-support interactions in single-atom catalysts. Angew Chem 2014; 126: 3486-3489. http://dx.doi.org/10.1002/ange.201309248

[6] Chen JY, Li GY, He ZG and An TC. Adsorption and degradation of model volatile organic compounds by a combined titania–montmorillonite–silica photocatalyst. J Hazard Mater 2011; 190: 416-423. http://dx.doi.org/10.1016/j.jhazmat.2011.03.064

[7] Li GY, Zhang ZY, Sun HW, Chen JY, An TC and Li B. Pollution profiles, health risk of VOCs and biohazards emitted from municipal solid waste transfer station and elimination by an integrated biological-photocatalytic flow system: A pilot-scale investigation. J Hazard Mater 2013; 250-251: 147-154. http://dx.doi.org/10.1016/j.jhazmat.2013.01.059

[8] An TC, Sun L, Li GY, Gao YP and Ying GG. Photocatalytic degradation and detoxification of *o*-chloroaniline in the gas phase: Mechanistic consideration and mutagenicity assessment of its decomposed gaseous intermediate mixture. Appl Catal B: Environ 2011; 102: 140-146. http://dx.doi.org/10.1016/j.apcatb.2010.11.035

[9] Chen JY, Liu XL, Li GY, Nie X, An TC, Zhang SQ, Zhao HJ. Synthesis and characterization of novel SiO_2 and TiO_2 co-pillared montmorillonite composite for adsorption and photocatalytic degradation of hydrophobic organic pollutants in water. Catal Today 2011; 164: 364-369. http://dx.doi.org/10.1016/j.cattod.2010.11.014

[10] An TC, Wan SG, Li GY, Sun L, Guo B. Comparison of the removal of ethanethiol in twin-biotrickling filters inoculated with strain RG-1 and B350 mixed microorganisms. J Hazard Mater 2010; 183: 372-380. http://dx.doi.org/10.1016/j.jhazmat.2010.07.035

[11] Li GY, Wan SG, An TC. Efficient bio-deodorization of aniline vapor in a biotrickling filter: Metabolic mineralization and bacterial community analysis. Chemosphere 2012; 87: 253-258. http://dx.doi.org/10.1016/j.chemosphere.2011.12.045

[12] Zekker I, Kroon K, Rikmann E, Tenno T, Tomingas M, Vabamäe P, Vlaeminck SE, Tenno T. Accelerating effect of hydroxylamine and hydrazine on nitrogen removal rate in moving bed biofilm reactor. Biodegradation 2012; 23: 739-749. http://dx.doi.org/10.1007/s10532-012-9549-6

[13] Zekker I, Rikmann E, Tenno T, Lemmiksoo V, Menert A, Loorits L, Vabamäe P, Tomingas M, Tenno T. Anammox enrichment from reject water on blank biofilm carriers and carriers containing nitrifying biomass: operation of two moving bed biofilm reactors (MBBR). Biodegradation 2012; 23: 547-560. http://dx.doi.org/10.1007/s10532-011-9532-7

[14] Zekker I, Rikmann E, Tenno T, Saluste A, Tomingas M, Menert A, Loorits L, Lemmiksoo V, Tenno T. Achieving nitritation and anammox enrichment in single moving-bed biofilm reactor treating reject water. Environ Technol 2012; 33: 703-710. http://dx.doi.org/10.1080/09593330.2011.588962

[15] Li FH, Fu XR, Huang J, Zhai JP. Synthesis of mesostructured iron oxides with potential As(V) adsorption application. Chem Res Chin Univ 2012; 28: 559-562.

[16] Sinha AK, Suzuki K. Three-dimensional mesoporous chromium oxide: A highly efficient material for the elimination of volatile organic compounds. Angew Chem 2005; 117: 275-277. http://dx.doi.org/10.1002/ange.200461284

[17] Sinha AK, Suzuki K. Novel mesoporous chromium oxide for VOCs elimination. Appl Catal B: Environ 2007; 70: 417-422. http://dx.doi.org/10.1016/j.apcatb.2005.10.035

[18] Ryoo R, Joo SH, Jun S. Synthesis of highly ordered carbon molecular sieves *via* template-mediated structural transformation. J Phys Chem B 1999; 103: 7743-7746. http://dx.doi.org/10.1021/jp991673a

[19] Bai BY, Arandiyan H, Li JH. Comparison of the performance for oxidation of formaldehyde on nano-Co_3O_4, 2D-Co_3O_4, and 3D-Co_3O_4 catalysts. Appl Catal B: Environ 2013; 142-143: 677-683. http://dx.doi.org/10.1016/j.apcatb.2013.05.056

[20] Xia YS, Dai HX, Jiang HY, Deng JG, He H, Au CT. Mesoporous chromia with ordered three-dimensional structures for the complete oxidation of toluene and ethyl acetate. Environ Sci Technol 2009; 43: 8355-8360. http://dx.doi.org/10.1021/es901908k

[21] Xia YS, Dai HX, Jiang HY, Zhang L, Deng JG, Liu YX. Three-dimensionally ordered and wormhole-like mesoporous iron oxide catalysts highly active for the oxidation of acetone and methanol. J Hazard Mater 2011; 186: 84-91. http://dx.doi.org/10.1016/j.jhazmat.2010.10.073

[22] Xia YS, Dai HX, Jiang HY, Zhang L. Three-dimensional ordered mesoporous cobalt oxides: Highly active catalysts for the oxidation of toluene and methanol. Catal Commun 2010; 11: 1171-1175. http://dx.doi.org/10.1016/j.catcom.2010.07.005

[23] Deng JG, Zhang L, Dai HX, Xia YS, Jiang HY, Zhang H, *et al*. Ultrasound- assisted nanocasting fabrication of ordered mesoporous MnO_2 and Co_3O_4 with high surface areas and polycrystalline walls. J Phys Chem C 2010; 114: 2694-2700. http://dx.doi.org/10.1021/jp910159b

[24] Xia YS, Dai HX, Zhang L, Deng JG, He H, Au CT. Ultrasound-assisted nanocasting fabrication and excellent catalytic performance of three- dimensionally ordered mesoporous chromia for the combustion of formaldehyde, acetone, and methanol. Appl Catal B: Environ 2010; 100: 229-237. http://dx.doi.org/10.1016/j.apcatb.2010.07.037

[25] Nair MM, Kleitz F, Kaliaguine S. Kinetics of methanol oxidation over mesoporous perovskite catalysts. ChemCatChem 2012; 4: 387-394. http://dx.doi.org/10.1002/cctc.201100356

[26] Gao BZ, Deng JG, Liu YX, Zhao ZX, Li XW, Wang Y, *et al*. Mesoporous $LaFeO_3$ catalysts for the oxidation of toluene and carbon monoxide. Chin J Catal 2013; 34: 2223-2229. http://dx.doi.org/10.1016/S1872-2067(12)60689-5

[27] Ying F, Wang SJ, Au CT, Lai SY. Highly active and stable mesoporous Au/CeO_2 catalysts prepared from MCM-48 hard-template. Microporous Mesoporous Mater 2011; 142: 308-315. http://dx.doi.org/10.1016/j.micromeso.2010.12.017

[28] Wang YF, Zhang CB, Liu FD, He H. Well-dispersed palladium supported on ordered mesoporous Co_3O_4 for catalytic oxidation of *o*-xylene. Appl Catal B: Environ 2013; 142-143: 72-79. http://dx.doi.org/10.1016/j.apcatb.2013.05.003

[29] Liu YX, Dai HX, Deng JG, Xie SH, Yang HG, Tan W, *et al*. Mesoporous Co_3O_4-supported gold nanocatalysts: Highly active for the oxidation of carbon monoxide, benzene, toluene, and *o*-xylene. J Catal 2014; 309: 408-418. http://dx.doi.org/10.1016/j.jcat.2013.10.019

[30] Ma CY, Mu Z, Li JJ, Jin YG, Cheng J, Lu GQ, *et al*. Mesoporous Co_3O_4 and Au/Co_3O_4 catalysts for low-temperature oxidation of trace ethylene. J Am Chem Soc 2010; 132: 2608-2613. http://dx.doi.org/10.1021/ja906274t

[31] Holland BT, Blanford CF, Stein A. Synthesis of macroporous minerals with highly ordered three-dimensional arrays of spheroidal voids. Science 1998; 281: 538-540. http://dx.doi.org/10.1126/science.281.5376.538

[32] Zhang J, Jin Y, Li CY, Shen YN, Han L, Hu ZX, *et al*. Creation of three-dimensionally ordered macroporous Au/CeO_2 catalysts with controlled pore sizes and their enhanced catalytic performance for formaldehyde oxidation. Appl Catal B: Environ 2009; 91: 11-20. http://dx.doi.org/10.1016/j.apcatb.2009.05.001

[33] Liu BC, Li CY, Zhang YF, Liu Y, Hu WT, Wang Q, *et al*. Investigation of catalytic mechanism of formaldehyde oxidation over three-dimensionally ordered macroporous Au/CeO_2 catalyst. Appl Catal B: Environ 2012; 111-112: 467-475. http://dx.doi.org/10.1016/j.apcatb.2011.10.036

[34] Liu Y, Liu BC, Wang Q, Li CY, Hu WT, Liu YX, *et al*. Three-dimensionally ordered macroporous Au/CeO_2–Co_3O_4 catalysts with mesoporous walls for enhanced CO preferential oxidation in H_2-rich gases. J Catal 2012; 296: 65-76. http://dx.doi.org/10.1016/j.jcat.2012.09.003

[35] Liu BC, Liu Y, Li CY, Hu WT, Jing P, Wang Q, *et al*. Three-dimensionally ordered macroporous Au/CeO_2−Co_3O_4 catalysts with nanoporous walls for enhanced catalytic oxidation of formaldehyde. Appl Catal B: Environ 2012; 127: 47-58. http://dx.doi.org/10.1016/j.apcatb.2012.08.005

[36] Xie SH, Deng JG, Zang SM, Yang HG, Guo GS, Arandiyan H, *et al*. Au–Pd/3DOM Co_3O_4: Highly active and stable nanocatalysts for toluene oxidation. J Catal 2015; 322: 38-48. http://dx.doi.org/10.1016/j.jcat.2014.09.024

[37] Li HN, Zhang L, Dai HX, He H. Facile synthesis and unique physicochemical properties of three-dimensionally ordered

macroporous magnesium oxide, gamma-alumina, and ceria-zirconia solid solutions with crystalline mesoporous walls. Inorg Chem 2009; 48: 4421-4434. http://dx.doi.org/10.1021/ic900132k

[38] Zhang RZ, Dai HX, Du YC, Zhang L, Deng JG, Xia YS, *et al*. P123–PMMA dual-templating generation and unique physicochemical properties of three-dimensionally ordered macroporous iron oxides with nanovoids in the crystalline walls. Inorg Chem 2011; 50: 2534-2544. http://dx.doi.org/10.1021/ic1023604

[39] Xie SH, Dai HX, Deng JG, Liu YX, Yang HG, Jiang Y, *et al*. Au/3DOM Co_3O_4: highly active nanocatalysts for the oxidation of carbon monoxide and toluene. Nanoscale 2013; 5: 11207-11219. http://dx.doi.org/10.1039/c3nr04126c

[40] Niu JR, Deng JG, Liu W, Zhang L, Wang GZ, Dai HX, *et al*. Nanosized perovskite-type oxides $La_{1-x}Sr_xMO_{3-\delta}$ (M = Co, Mn; x = 0, 0.4) for the catalytic removal of ethylacetate. Catal Today 2007; 126: 420-429. http://dx.doi.org/10.1016/j.cattod.2007.06.027

[41] Deng JG, Dai HX, Jiang HY, Zhang L, Wang GZ, He H, *et al*. Hydrothermal fabrication and catalytic properties of $La_{1-x}Sr_xM_{1-y}Fe_yO_3$ (M = Mn, Co) that are highly active for the removal of toluene. Environ Sci Technol 2010; 44: 2618-2623. http://dx.doi.org/10.1021/es9031997

[42] Deng JG, Zhang L, Dai HX, He H, Au CT. Strontium-doped lanthanum cobaltite and manganite: Highly active catalysts for toluene complete oxidation. Ind Eng Chem Res 2008; 47: 8175-8183. http://dx.doi.org/10.1021/ie800585x

[43] Deng JG, Zhang L, Dai HX, He H, Au CT, Single-crystalline $La_{0.6}Sr_{0.4}CoO_{3-\delta}$ nanowires/nanorods derived hydrothermally without the use of a template: Catalysts highly active for toluene complete oxidation. Catal Lett 2008; 123: 294-300. http://dx.doi.org/10.1007/s10562-008-9422-8

[44] Deng JG, Zhang Y, Dai HX, Zhang L, He H, Au CT. Effect of hydrothermal treatment temperature on the catalytic performance of single-crystalline $La_{0.5}Sr_{0.5}MnO_{3-\delta}$ microcubes for the combustion of toluene. Catal Today 2008; 139: 82-87. http://dx.doi.org/10.1016/j.cattod.2008.08.010

[45] Deng JG, Zhang L, Dai HX, He H, Au CT. Hydrothermally fabricated single-crystalline strontium-substituted lanthanum manganite microcubes for the catalytic combustion of toluene. J Mol Catal A: Chem 2009; 299: 60-67. http://dx.doi.org/10.1016/j.molcata.2008.10.006

[46] Sadakane M, Asanuma T, Kubo J, Ueda W. Facile procedure to prepare three-dimensionally ordered macroporous (3DOM) perovskite-type mixed metal oxides by colloidal crystal templating method. Chem Mater 2005; 17: 3546-3551. http://dx.doi.org/10.1021/cm050551u

[47] Liu YX, Dai HX, Deng JG, Zhang L, Au CT. Three-dimensional ordered macroporous bismuth vanadates: PMMA-templating fabrication and excellent visible light-driven photocatalytic performance for phenol degradation. Nanoscale 2012; 4: 2317-2325. http://dx.doi.org/10.1039/c2nr12046a

[48] Wang Y, Dai HX, Deng JG, Liu YX, Zhao ZX, Li XW, *et al*. Three-dimensionally ordered macroporous $InVO_4$: Fabrication and excellent visible-light-driven photocatalytic performance for methylene blue degradation. Chem Eng J 2013; 226: 87-94. http://dx.doi.org/10.1016/j.cej.2013.04.032

[49] Liu YX, Dai HX, Deng JG, Zhang L, Zhao Z X, Li XW, *et al*. Controlled generation of uniform spherical $LaMnO_3$, $LaCoO_3$, Mn_2O_3, and Co_3O_4 nanoparticles and their high catalytic performance for carbon monoxide and toluene oxidation. Inorg Chem 2013; 52: 8665-8676. http://dx.doi.org/10.1021/ic400832h

[50] Liu YX, Dai HX, Deng JG, Zhang L, Gao BZ, Wang Y, *et al*. PMMA-templating generation and high catalytic performance of chain-like ordered macroporous $LaMnO_3$ supported gold nanocatalysts for the oxidation of carbon monoxide and toluene. Appl Catal B: Environ 2013; 140-141: 317-326. http://dx.doi.org/10.1016/j.apcatb.2013.04.025

[51] Liu YX, Dai HX, Du YC, Deng JG, Zhang L, Zhao ZX, *et al*. Controlled preparation and high catalytic performance of three-dimensionally ordered macroporous $LaMnO_3$ with nanovoid skeletons for the combustion of toluene. J Catal 2012; 287: 149-160. http://dx.doi.org/10.1016/j.jcat.2011.12.015

[52] Liu YX, Dai HX, Deng JG, Li XW, Wang Y, Arandiyan H, *et al*. Au/3DOM $La_{0.6}Sr_{0.4}MnO_3$: Highly active nanocatalysts for the oxidation of carbon monoxide and toluene. J Catal 2013; 305: 146-153. http://dx.doi.org/10.1016/j.jcat.2013.04.025

[53] Ji KM, Dai HX, Deng JG, Song LY, Gao BZ, Wang Y, *et al*. Three-dimensionally ordered macroporous $Eu_{0.6}Sr_{0.4}FeO_3$ supported cobalt oxides: Highly active nanocatalysts for the combustion of toluene. Appl Catal B: Environ 2013; 129: 539-548. http://dx.doi.org/10.1016/j.apcatb.2012.10.005

[54] Li XW, Dai HX, Deng JG, Liu YX, Zhao ZX, Wang Y, *et al*. In situ PMMA-templating preparation and excellent catalytic performance of Co_3O_4/3DOM $La_{0.6}Sr_{0.4}CoO_3$ for toluene combustion. Appl Catal A: Gen 2013; 458: 11-20. http://dx.doi.org/10.1016/j.apcata.2013.03.022

[55] Jiang Y, Deng JG, Xie SH, Yang HG, Dai HX. Au/MnO_x/3DOM $La_{0.6}Sr_{0.4}MnO_3$: Highly active nanocatalysts for the complete oxidation of toluene. Ind Eng Chem Res 2015; 54: 900-910. http://dx.doi.org/10.1021/ie504304u

[56] Liu YX, Dai HX, Du YC, Deng JG, Zhang L, Zhao ZX. Lysine-aided PMMA-templating preparation and high performance of three-dimensionally ordered macroporous $LaMnO_3$ with mesoporous walls for the catalytic combustion of toluene. Appl Catal B: Environ 2012; 119-120: 20-31. http://dx.doi.org/10.1016/j.apcatb.2012.02.010

[57] Ji KM, Dai HX, Deng JG, Zhang L, Wang F, Jiang HY, *et al*. Three-dimensionally ordered macroporous $SrFeO_{3-\delta}$ with high surface area: Active catalysts for the complete oxidation of toluene. Appl Catal A: Gen 2012; 425-426: 153-160. http://dx.doi.org/10.1016/j.apcata.2012.03.013

[58] Ji KM, Dai HX, Dai JX, Deng JG, Wang F, Zhang H, *et al*. PMMA-templating preparation and catalytic activities of three-dimensional macroporous strontium ferrites with high surface areas for toluene combustion. Catal Today 2013; 201: 40-48. http://dx.doi.org/10.1016/j.cattod.2012.03.061

[59] Ji KM, Dai HX, Deng JG, Jiang HY, Zhang H, Cao YJ. Catalytic removal of toluene over three-dimensionally ordered macroporous $Eu_{1-x}Sr_xFeO_3$. Chem Eng J 2013; 214: 262-271. http://dx.doi.org/10.1016/j.cej.2012.10.083

[60] Zhao ZX, Dai HX, Deng JG, Du YC, Liu YX, Zhang L. Three-dimensionally ordered macroporous $La_{0.6}Sr_{0.4}FeO_{3-\delta}$: High-efficiency catalysts for the oxidative removal of toluene. Micropor Mesopor Mater 2012; 163: 131-139. http://dx.doi.org/10.1016/j.micromeso.2012.07.006

[61] Zhao ZX, Dai HX, Deng JG, Du YC, Liu YX, Zhang L. Preparation of three-dimensionally ordered macroporous $La_{0.6}Sr_{0.4}Fe_{0.8}Bi_{0.2}O_{3-\delta}$ and their excellent catalytic performance for the combustion of toluene. J Mol Catal A: Chem 2013; 366: 116-125. http://dx.doi.org/10.1016/j.molcata.2012.09.014

[62] Ji KM, Dai HX, Deng JG, Li XW, Wang Y, Gao BZ, *et al*. A comparative study of bulk and 3DOM-structured Co_3O_4, $Eu_{0.6}Sr_{0.4}FeO_3$, and Co_3O_4/$Eu_{0.6}Sr_{0.4}FeO_3$: Preparation, characterization, and catalytic activities for toluene

combustion. Appl Catal A: Gen 2012**;** 447-448: 41-48. http://dx.doi.org/10.1016/j.apcata.2012.09.004

[63] Liu YX, Dai HX, Deng JG, Du YC, Li XW, Zhao ZX, *et al*. In situ poly(methyl methacrylate)-templating generation and excellent catalytic performance of MnO_x/3DOM $LaMnO_3$ for the combustion of toluene and methanol. Appl Catal B: Environ 2013; 140-141: 493-505. http://dx.doi.org/10.1016/j.apcatb.2013.04.051

[64] Li XW, Dai HX, Deng JG, Liu YX, Xie SH, Zhao ZX, *et al*. Au/3DOM $LaCoO_3$: High-performance catalysts for the oxidation of carbon monoxide and toluene. Chem Eng J 2013; 228: 965-975. http://dx.doi.org/10.1016/j.cej.2013.05.070

Received on 02-05-2015 Accepted on 19-05-2015 Published on 14-07-2015

DOI: http://dx.doi.org/10.15377/2410-3624.2015.02.01.1